crystals

MDPI

Article

Shifts in Backbone Conformation of Acetylcholinesterases upon Binding of Covalent Inhibitors, Reversible Ligands and Substrates

Zoran Radić

Skaggs School of Pharmacy and Pharmaceutical Sciences, University of California San Diego, La Jolla, CA 92093-0751, USA; zradic@ucsd.edu

Abstract: The influence of ligand binding to human, mouse and *Torpedo californica* acetylcholinesterase (EC 3.1.1.7; AChE) backbone structures is analyzed in a pairwise fashion by comparison with X-ray structures of unliganded AChEs. Both complexes with reversible ligands (substrates and inhibitors) as well as covalently interacting ligands leading to the formation of covalent AChE conjugates of tetrahedral and of trigonal-planar geometries are considered. The acyl pocket loop (AP loop) in the AChE backbone is recognized as the conformationally most adaptive, but not necessarily sterically exclusive, structural element. Conformational changes of the centrally located AP loop coincide with shifts in C-terminal α-helical positions, revealing interacting components for a potential allosteric interaction within the AChE backbone. The stabilizing power of the aromatic choline binding site, with the potential to attract and pull fitting entities covalently tethered to the active Ser, is recognized. Consequently, the pull can promote catalytic reactions or relieve steric pressure within the impacted space of the AChE active center gorge. These dynamic properties of the AChE backbone inferred from the analysis of static X-ray structures contribute towards a better understanding of the molecular template important in the structure-based design of therapeutically active molecules, including AChE inhibitors as well as reactivators of conjugated, inactive AChE.

Keywords: acetylcholinesterase; organophosphate; carbamate; backbone conformation; oxime reactivation; oxime antidote; acetylcholine

Citation: Radić, Z. Shifts in Backbone Conformation of Acetylcholinesterases upon Binding of Covalent Inhibitors, Reversible Ligands and Substrates. *Crystals* **2021**, *11*, 1557. https://doi.org/10.3390/cryst11121557

Academic Editor: Abel Moreno

Received: 1 December 2021
Accepted: 11 December 2021
Published: 14 December 2021

1. Introduction

Acetylcholinesterase (EC 3.1.1.7; AChE) is an essential regulatory enzyme in cholinergic neurotransmission of vertebrates. It has evolved, consistent with its important function, into near-perfect biological catalyst [1]. The high catalytic throughput in the hydrolysis of the neurotransmitter acetylcholine (ACh) is achieved owing to the specific three-dimensional structure of its catalytic subunit. Whether completion of the catalytic cycle in AChE depends on conformational adjustments in its structure is an open question.

Because of the size of the ~70 kDa catalytic subunit, only approaches capable of resolving "static" structural snapshots have been successful in obtaining atomic structures of AChE [2]. Those structural snapshots, documented in more than 200 PDB-deposited X-ray structures, have not revealed any significant conformational outliers and seem to largely reveal one dominant conformation of the backbone [3]. Several smaller conformational deviations have been identified, however. Most of them have been associated with the AChE acyl pocket loop [4,5]. Because macromolecular structural dynamics and the catalytic activity of AChE can be detected even in the crystalline state [6,7], analysis of low-level conformational diversity in AChE X-ray structures could provide a glimpse of a larger-scale flexibility requirement for physiological function in solution.

Catalytic specificities of cholinesterases, both AChE and that of the closely related butyrylcholinesterase (EC 3.1.1.8; BChE), have been previously defined to depend on the size and ligand-binding capacity of three enzyme domains: the acyl pocket, the choline

binding site and the peripheral site [8]. We have recently revealed, however, that the size of the acyl pocket in human AChE (hAChE) has to be used with caution as a sole criterion for the specificity [9]. We have shown that some of large organophosphate (OP) substrates of hAChE, such as Novichok A234, contrary to expectation, insert their ethoxy substituent on phosphorus into the hAChE acyl pocket and fit the overall active center without notable distortions of the hAChE backbone [9] or its side-chains.

In here, the presented analysis of complexes and conjugates of AChEs is expanded to include those with carboxylic and carbamic ester substrates in addition to OPs. Furthermore, in addition to the structure of hAChE, the structures of mouse AChE (mAChE) and Torpedo californica AChE (TcAChE) have been analyzed. In a pairwise fashion, the PDB-deposited X-ray structures of native AChEs have been compared to those of their carbamylated conjugates, OP-hAChE conjugates as well as of those reversibly complexed with carboxylic acid substrates, hydrolytic products and some of the tight binding reversible inhibitors. The Pairwise Alpha Carbon Comparison Tool (PACCT 3) was used for comparisons (www.ZENODO.org, doi:10.5281/zenodo.3992329. Last access on 30 November 2021), as presented earlier [9–12].

2. Materials and Methods

X-ray structures of hAChE, mAChE and TcAChE in their unliganded, apo forms, covalently inhibited by OPs or carbamates, in reversible complexes with the substrates ACh, acetylthiocholine (ATCh), butyrylthiocholine (BTCh), hydrolytic products choline (Ch), thiocholine (TCh) and acetate (Ac) and with tight binding reversible inhibitors, were obtained from the RCSB PDB database [13]. The frames of reference in pairwise structural comparisons were the structures of unliganded (apo) AChEs; this was, specifically, PDB ID 4EY4 for hAChE [14], PDB ID 1J06 for mAChE [6] and PDB ID 2ACE for TcAChE [2].

The Pairwise Alpha Carbon Comparison Tool (PACCT 3) used for pairwise comparisons of α-carbon positions/shifts in structural backbones is available for download from Zenodo (www.ZENODO.org, doi:10.5281/zenodo.3992329. Last access on 30 November 2021), and was used as shown earlier [9–12]. A bar chart PACCT 3 output of shifts in backbone Cα positions (given in Å) was used for comparison as a function of amino acid residue number. For each of the analyzed structures, unless otherwise indicated, chain A was compared to the chain A of the respective apo-AChE. The resulting bar chart was overlaid with charts of other relevant structures in question. Average Cα shift values were indicated in bar charts for each of the inter-structural comparisons as horizontal dashed lines. Peaks of Cα shifts extending above the inter-structural average were taken as significant. The exceptions were peaks observed at the C- and N-termini and around breaks (missing parts of compared structures).

For the visual analysis of the structures in this comparison, PACCT 3-generated overlays were used and visualized in the VR-based visualization suite Nanome (Nanome Inc., San Diego, CA, USA). Overlays were based on the superposition of twenty Cα atom coordinates with the smallest observed values of Cα shifts in the respective comparison.

3. Results

3.1. Effects of Covalent Binding on Backbone Conformation of hAChE

3.1.1. Reversible, Covalent Binding of the Substrate Analogue 4KTMA

Pairwise analyses of covalent conjugates of the hemiketal 4KTMA (Figure 1A) with hAChE, mAChE and TcAChE, in comparison to structures of their corresponding apo forms, do not reveal any significant backbone distortions (Figure 1). Only small ~0.2 Å Cα shifts could be observed in the more N-terminal part of the Ω loop and in the C-terminally located α-helix II in all 3 AChEs (Figure 1B). The bound 4KTMA entity fills and fits well in the lower part of the active center gorge between the acyl pocket and the choline binding site. Its geometry mimics the tetrahedral transition state in the hydrolytic cycle of ACh. The similarity of conjugated backbone conformations with those of apo AChEs suggest that active center geometries of native, apo hAChEs appear quite adequate for achieving

fast catalytic turnovers of the bound physiological substrate without additional substrate-induced adjustments.

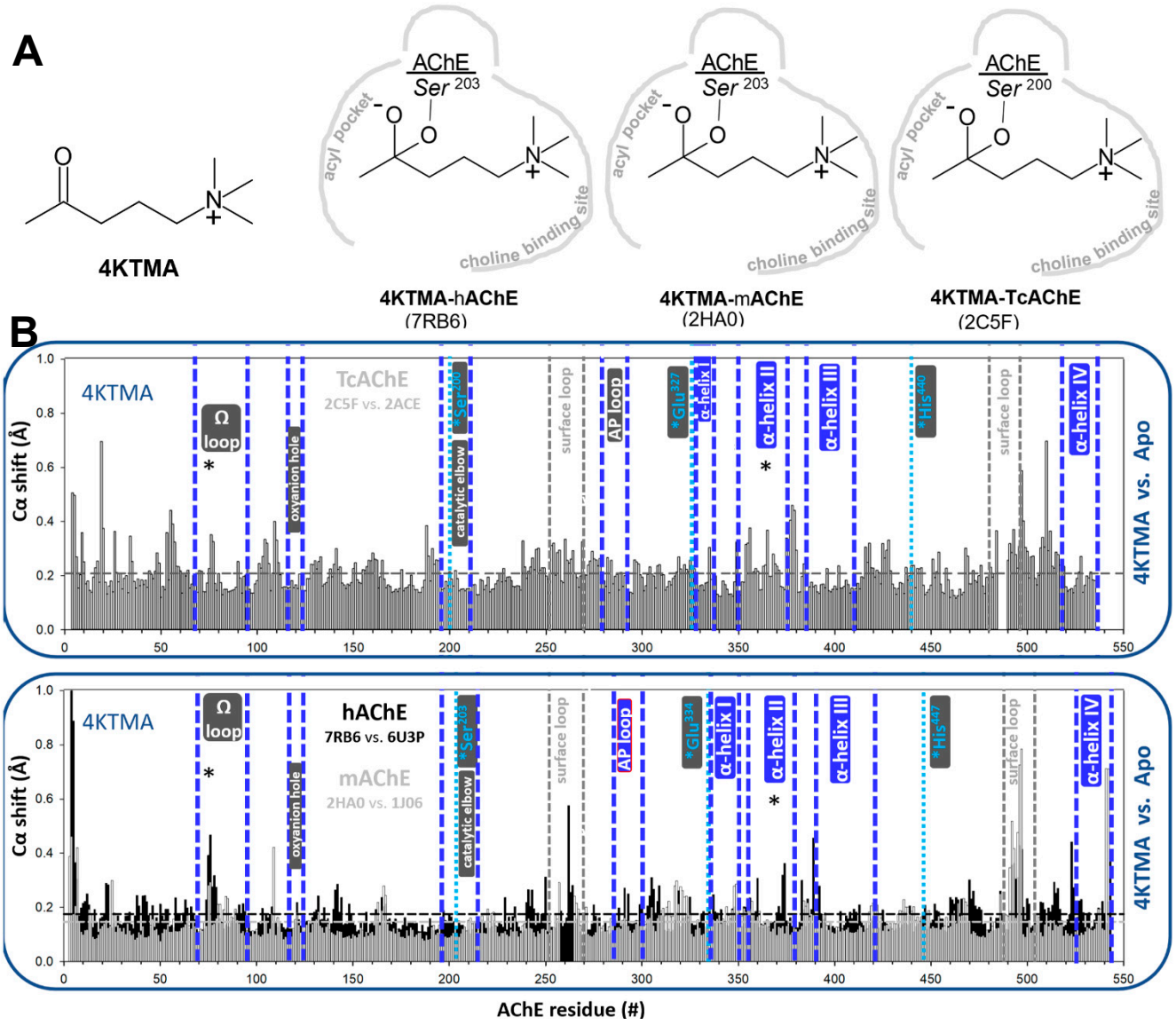

Figure 1. (**A**) Structure of the substrate analogue 4KTMA and schematic representation of its binding to the active serine within the active centers of three AChEs based on X-ray structures with PDB codes given in parentheses. (**B**) Bar charts from PACCT3 analyses of each of the three conjugate structures compared to the corresponding apo AChE forms. Alpha carbon shifts (in Å) of conjugated backbones are represented as vertical bars for each amino acid in the linear AchE sequence. Horizontal dashed lines indicate an average backbone atom shift, while stars indicate shifts considered as significant. Functionally important structural elements of AChE are bracketed between vertical, dashed, and blue lines and labelled. Their location within the 3D structure of AChE is shown in Figure 2.

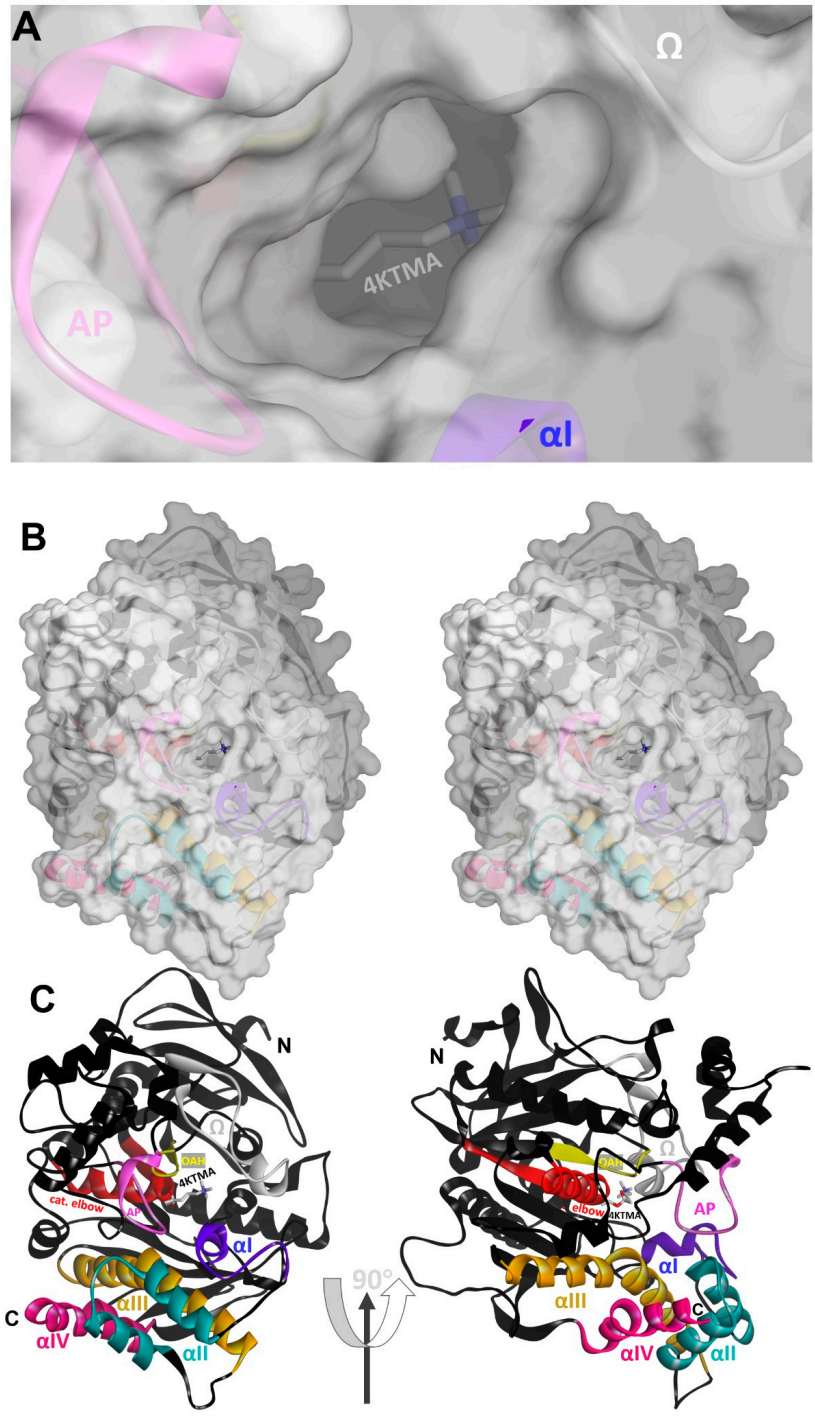

Figure 2. Locations of structural elements of the hAChE backbone affected by covalent or reversible ligand binding as detected by PACCT 3 analysis. (**A**) Close-up of the active center gorge opening in the 4KTMA-hAChE conjugate (PDB ID 7RB6). Semi-transparent Connolly surface presentation. (**B**) Stereo view of the catalytic subunit. The semi-transparent surface reveals Cα ribbon color coded by structural elements and in the same view as in the (**C**) **Left panel:** showing AP loop (286–299; pink), Ω-loop (69–96; gray), oxyanion hole (117–124; yellow), catalytic elbow (196–215; red), α-helices I (336–350; blue), II (356–382; teal), III (390–421) orange), and IV (525–543; magenta). (**C**) **Right panel:** the same color-coded elements in ribbon, rotated clockwise by 90°. Covalently bound 4KTMA is rendered as sticks.

In particular, conformations of three loops that control the size of the active center opening (AP loop, Ω loop and α-helix I; cf. Figure 2) do not seem to be influenced in the tetrahedral 4KTMA conjugate (Figure 1B) in any concerted manner.

3.1.2. Covalent Conjugates Formed by OPs

Tetrahedral conjugates formed by covalent binding of OPs have the capacity to significantly influence backbone conformations of AChEs, as already noted for hAChE [9]. One of two ethoxy groups of diethylphosphorylated hAChE, formed by POX inhibition, has to be accommodated in the small acyl pocket of AChE resulting in a large distortion of the AP loop (Figure 3). This was observed in both of two different POX-hAChE X-ray structure datasets (5HF5 and 5HF8), but also in the structure of the smaller, dealkylated (aged) POX-hAChE conjugate (5HF6). The two-point attachment of those conjugates, one by covalent bond to Ser203 and two by tight stabilization of the phosphonyl oxygen in the oxyanion hole, should, however, still allow for a shift of a conjugate towards the empty space of the choline binding site in order to relieve the steric AP loop pressure, but that is not observed in these X-ray structures. Additionally, no backbone shifts are observed around two attachment points, the oxyanion hole and Ser203 (Figure 3), indicating no tendency for the conjugate to shift in spite of the availability of the space within the active center gorge for that shift. It seems that the distorted AP loop is not forcing the offending ethoxy group out of the acyl pocket in order to resume its native conformation. This possibly reflects a small energetic difference between a variety of conformations of this loop and speaks of the freedom of its intrinsic conformational flexibility.

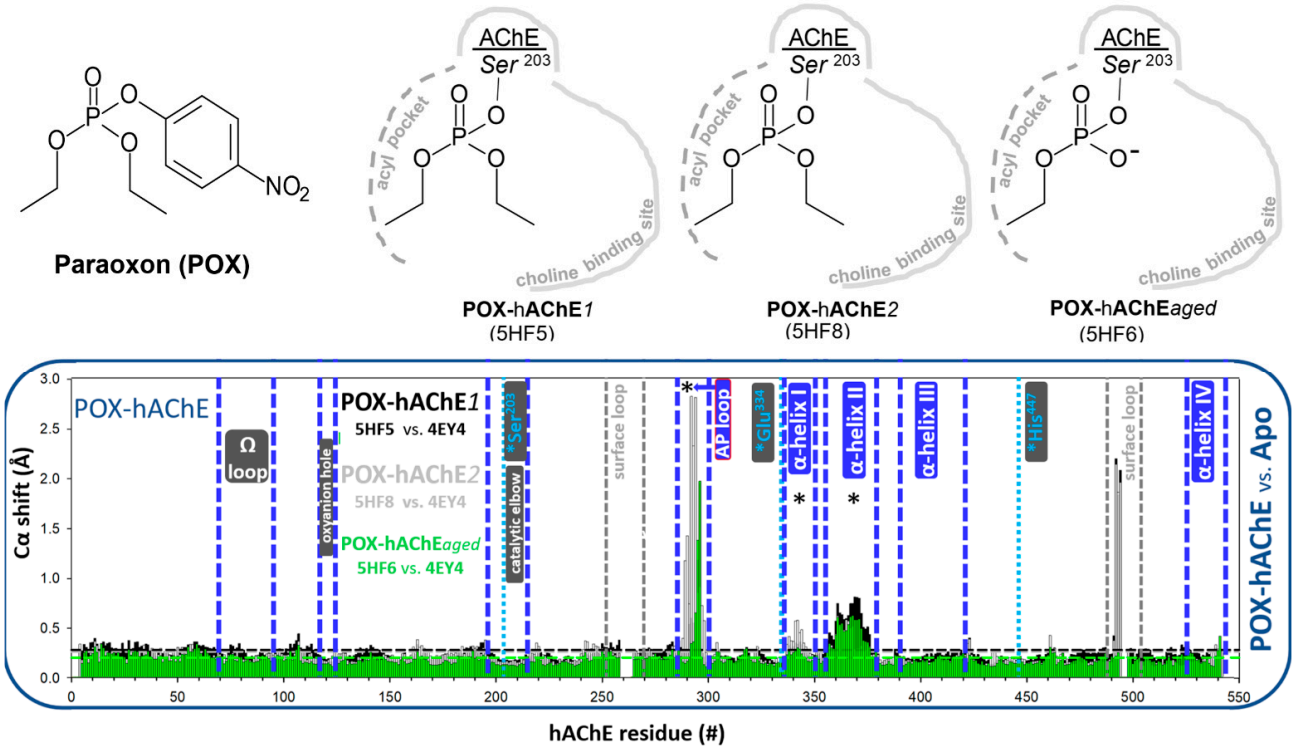

Figure 3. Structure of paraoxon (POX), an active form of the pesticide parathion, and schematic representation of its covalent binding to the active serine of hAChE in two conformationally different covalent conjugates and in the aged (dealkylated) form. Schematics are based on X-ray structures with PDB codes given in parentheses. Bar charts from PACCT3 analyses of each of 3 structures compared to the apo AChE (4EY4). Alpha carbon shifts (in Å) of conjugated backbones are represented as vertical bars for each amino acid in the linear AChE sequence. Horizontal dashed lines indicate an average backbone atom shift, while stars indicate shifts considered as significant. Functionally important structural elements of hAChE, bracketed between vertical, dashed, and blue lines and labelled, are mapped within the 3D structure of the hAChE in Figure 2.

We recently suggested [9] that substituents on phosphorus capable of forming stabilizing interactions with the choline binding site (hydrophobic or electrostatic) can pull the respective conjugate away from the acyl pocket and allow the AP loop to recover its native conformation. In fact, a similar effect can be observed even when the acyl pocket-binding substituent is small and fits inside the AP pocket well, such as in the absence of steric clashes within the AP (Figure 4). For example, the binding of neither the methyl phosphonates, VX, soman or A230 distorts the AP loop (Figure 4). The P atom in those conjugates is, however, consistently pulled towards the choline binding site by virtue of hydrophobic and electrostatic attractions of the large choline binding site interacting with substituents in soman and A230. Phosphorus atoms in the conjugates of large soman and A230 are shifted by 0.5–0.6 Å compared to the much smaller VX.

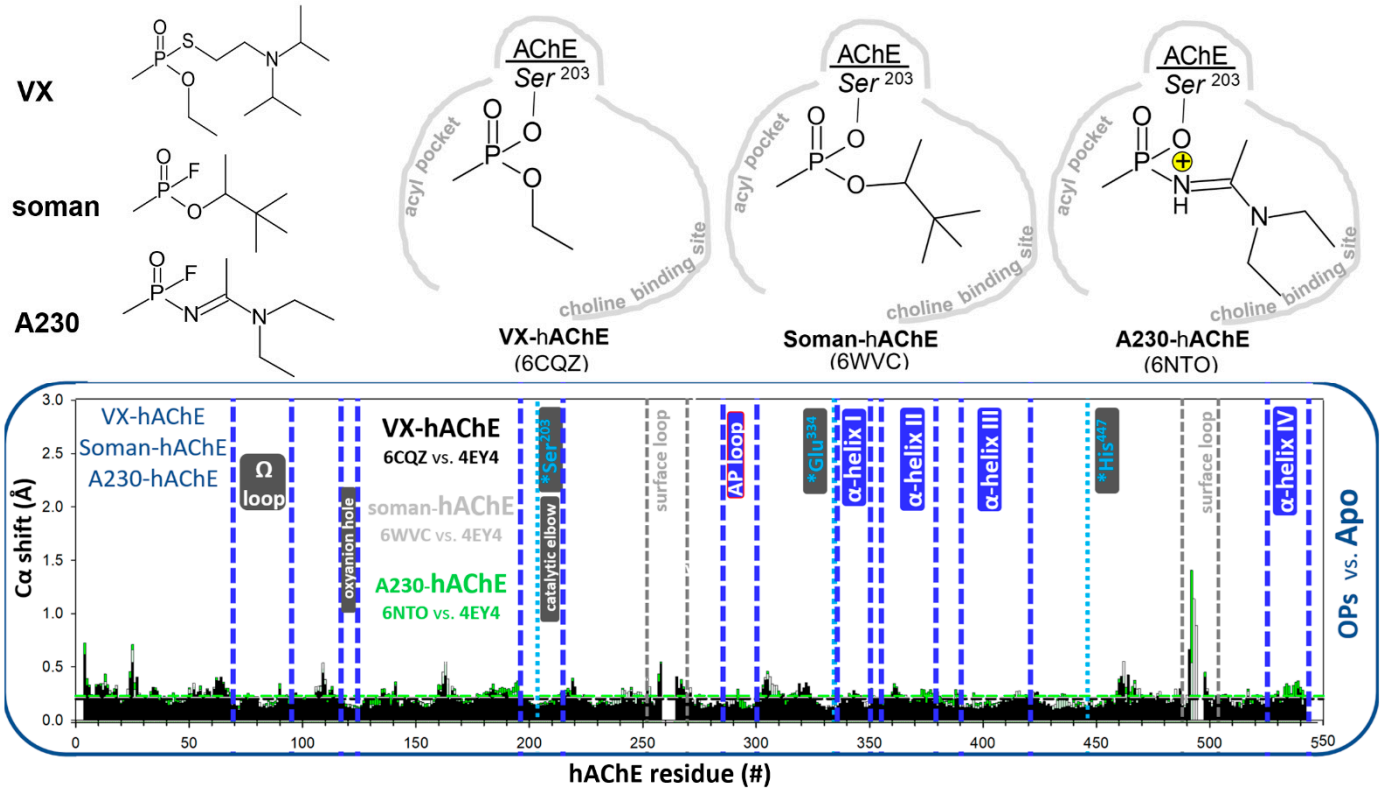

Figure 4. The structure of the nerve agents OPs, VX, soman and A230 and a schematic representation of their covalent binding to the active serine of hAChE. Schematics are based on X-ray structures with PDB codes given in parentheses. Bar charts from PACCT3 analyses of each of the three structures compared to the apo AChE (4EY4). Alpha carbon shifts (in Å) of conjugated backbones are represented as vertical bars for each amino acid in the linear AChE sequence. Horizontal dashed lines indicate an average backbone atom shift, while stars indicate shifts considered significant. Functionally important structural elements of hAChE, bracketed between vertical, dashed, and blue lines and labelled, are mapped within the 3D structure of hAChE in Figure 2.

The AP loop distortions seem to clearly coincide with shifts of the α-helix II, and to a smaller extent, the α-helix I (Figure 3). In the absence of the AP loop distortion, α-helices I and II do not shift (Figure 4). Those helices are within 5–6 Å of the AP loop, allowing for a direct interaction leading to conformational connectivity. This kind of connectivity between the active center and C-terminal α-helices of the hAChE homodimer interface is likely responsible for the POX-triggered dissociation of the hAChE homodimer, observed in solution using SAXS [11], indicating connectivity between the AP loop distortion and disturbance at the homodimer interface of hAChE.

In this context, it is also instructive to analyze differences in backbone conformations of OP-hAChE conjugates obtained by the inhibition of separate enantiomers of VX, S_PVX-

hAChE (6CQZ) and R_PVX-hAChE (6CQX), since inhibition of hAChE by an R_P isomer of sarin (unlike the S_P isomer) was shown to have a similar effect on the homodimer dissociation as POX [11]. The enantiomeric S_PVX-hAChE conjugate was obtained by inhibition of racemic VX, due to the about two orders of magnitude faster rate of inhibition by the S_P enantiomer [15]. Indeed, consistent with AP loop distortions observed in the POX-hAChE conjugate (Figure 3), the R_PVX-hAChE structure showed both AP loop distortion and shifts in α-helices II and I, while none of those effects were observed in the structure of the S_PVX-hAChE conjugate (Figure 5). The enantio-specific effect is very clear in spite of some differences in the AP loop conformations in chains A and B of the R_PVX-hAChE (Figure 5), which in fact reflects its intrinsic conformational flexibility.

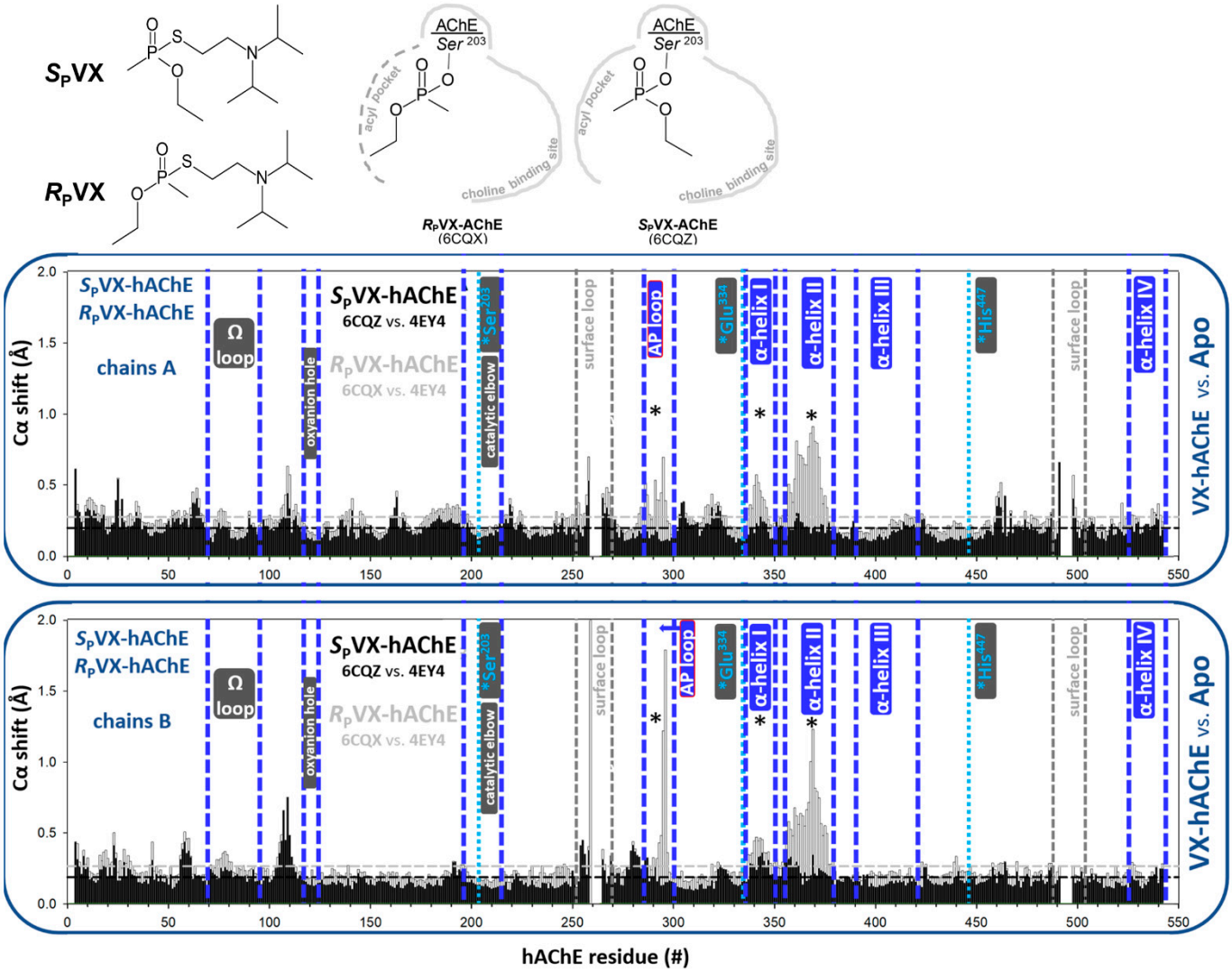

Figure 5. Structure of enantiomers of VX, and schematic representation of their covalent binding to the active serine of hAChE. Schematics are based on X-ray structures with PDB codes given in parentheses. Bar charts from PACCT3 analyses of each of three structures compared to the apo AChE (4EY4). Alpha carbon shifts (in Å) of conjugated backbones are represented as vertical bars for each amino acid in the linear AChE sequence. Horizontal dashed lines indicate an average backbone atom shift, while stars indicate shifts considered significant. Functionally important structural elements of hAChE, bracketed between vertical, dashed, and blue lines and labelled, are mapped within the 3D structure of hAChE in Figure 2.

Another commonly used symmetric OP, DFP (Figure 6), forms conjugates with AchEs where the AP loop is distorted upon the insertion of one of its two large isopropoxy substituents on phosphorus. It has been well described that DFP-AChEs age (dealkylate)

in minutes to hours [16]. Available X-ray structures of both non-aged and aged DFP-AChE conjugates with mAChE and aged DFP-TcAChE conjugate reveal large distortions of their AP loops (Figure 6). Magnitudes of backbone Cα shifts appear similar to the ones inflicted by POX. The two different X-ray datasets of the aged DFP-mAChE (2JGM and 5HCU) differ somewhat in their extent of distortion, yet distortion is observed in both, along with associated shifts of α helices II and I (Figure 6). Furthermore, in one of the structures of the aged conjugate, the dealkylated group was shown to be stabilized within the AP (5HCU). This is somewhat surprising, considering the accepted mechanism of aging, where amino acid residues involved in the stabilization of carbonium cations in the course of dealkylation are the choline binding site residues F338 and E202 [16]. Interestingly, reversible binding of non-oxime reactivating antidote SP-134 stabilized one very distorted AP loop conformation upon its insertion into an already distorted acyl pocket of the aged DFP-mAChE (Figure 6). This effect is opposite from what is observed upon binding of pyridinium oxime reactivators HI-6 and/or 2PAM to POX-hAChE, where reversal of the distorted AP loop conformations into native conformations was shown [9]. The likely reason for the difference is that pyridinium oximes bind within the main cavity of the active center gorge of POX-hAChE without entering into the acyl pocket.

Conjugation of an AChE with tabun can also lead to distortion of the AP loop, but under slightly more complicated conditions. This was demonstrated recently in X-ray structures of TcAChE conjugated by NEDPA, an analog of tabun that forms identical conjugates with TcAChE [5]. The dimethylamino group in those conjugates (6G17 for Tabun or 6G4O; chain B for NEDPA conjugates) is always accommodated in the acyl pocket of the undisturbed, native conformation, while the larger ethoxy group points towards the choline binding site. Only reversible binding of novel uncharged aldoximes R1 or R2 to the conjugate was shown to have the capacity to distort the AP loop conformation. The structures of R1 and R2 are very similar [5]. Both reactivators were shown to distort only one of two monomers in the crystallographic homodimer of released structures. For R2, binding to chain A did not cause distortion, though it did for the chain B. On the other hand, R1 was found bound to only chain A where the AP loop was distorted, and chain B was free from both R1 binding and distortion (Figure 7). Those observations illustrate small magnitudes of energy barriers in the conformational flexibility of the AP loop, where reversibly bound R2 can, but does not have to, promote loop distortion. Both R1 and R2 bind to the same area of the peripheral site in TcAChE and in very similar orientations, where they interact directly with the concave parts of the AP loop. Furthermore, a significant observation related to the connectivity of the structural elements of TcAChE is that distortion of the AP loop always coincides with backbone shifts of α-helix II. When the AP loop is in its native conformation (no peaks in the bar chart in the AP loop area), no shifts (no peaks in bar charts) can be observed for α-helix II, as well (Figure 6). This seems to be a common connectivity pattern for both hAChE, mAChE and TcAChE.

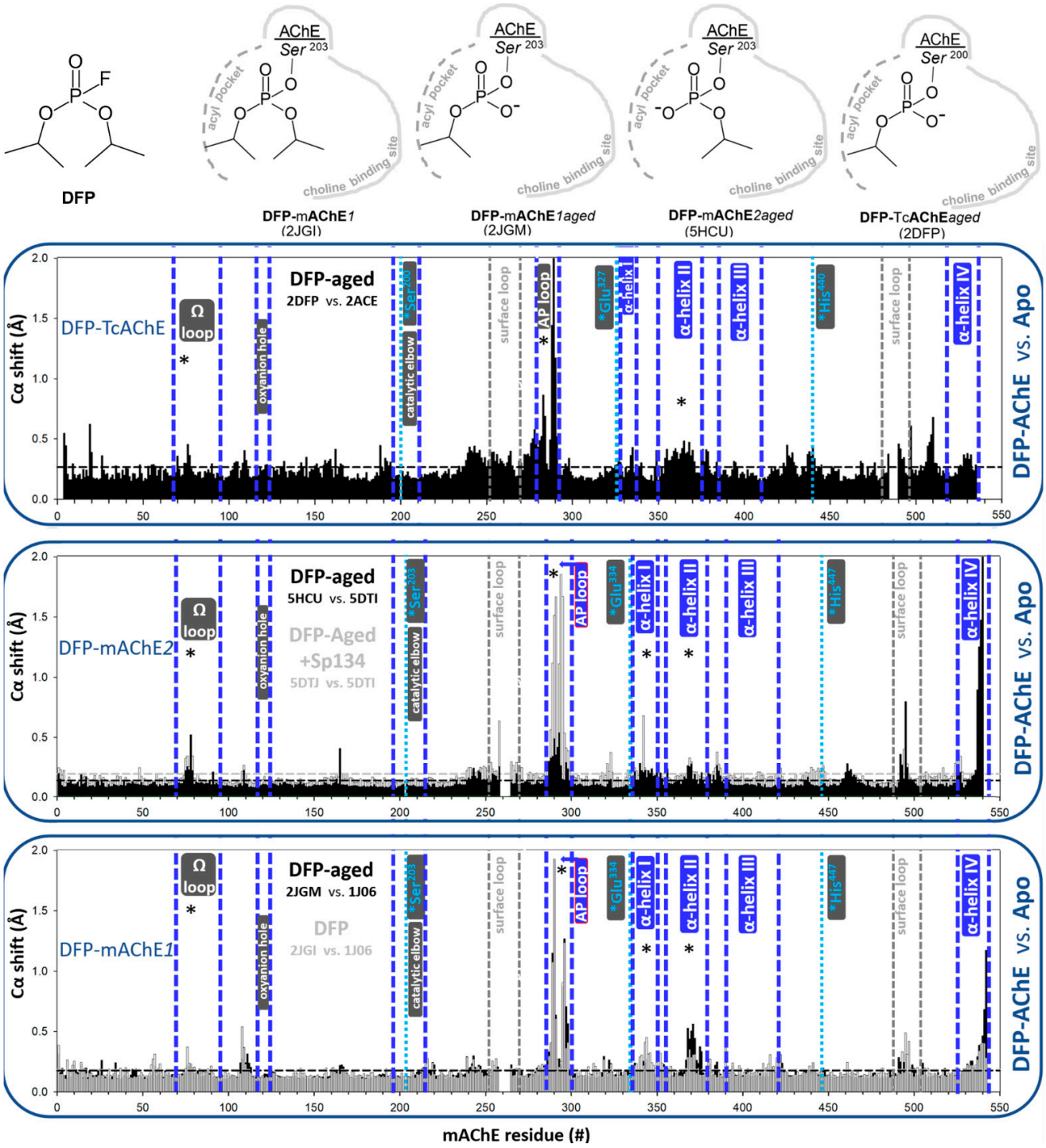

Figure 6. Structure of DFP and schematic representation of its covalent binding to the active serine of TCAChE and mAChE in aged (dealkylated) and non-aged forms. Schematics are based on one aged DFP-TcAChE and two sets of X-ray structures of DFP-mAChE with PDB codes given in parentheses. One of these structures refers to the reversible complex of aged DFP-mAChE with reactivator Sp134. Bar charts from PACCT3 analyses of each of these three structures compared to the corresponding apo AChEs. Alpha carbon shifts (in Å) of conjugated backbones are represented as vertical bars for each amino acid in the linear AChE sequence. Horizontal dashed lines indicate an average backbone atom shift, while stars indicate shifts considered significant. Functionally important structural elements of hAChE, bracketed between vertical, dashed, and blue lines and labelled, are mapped in the 3D structure of hAChE in Figure 2.

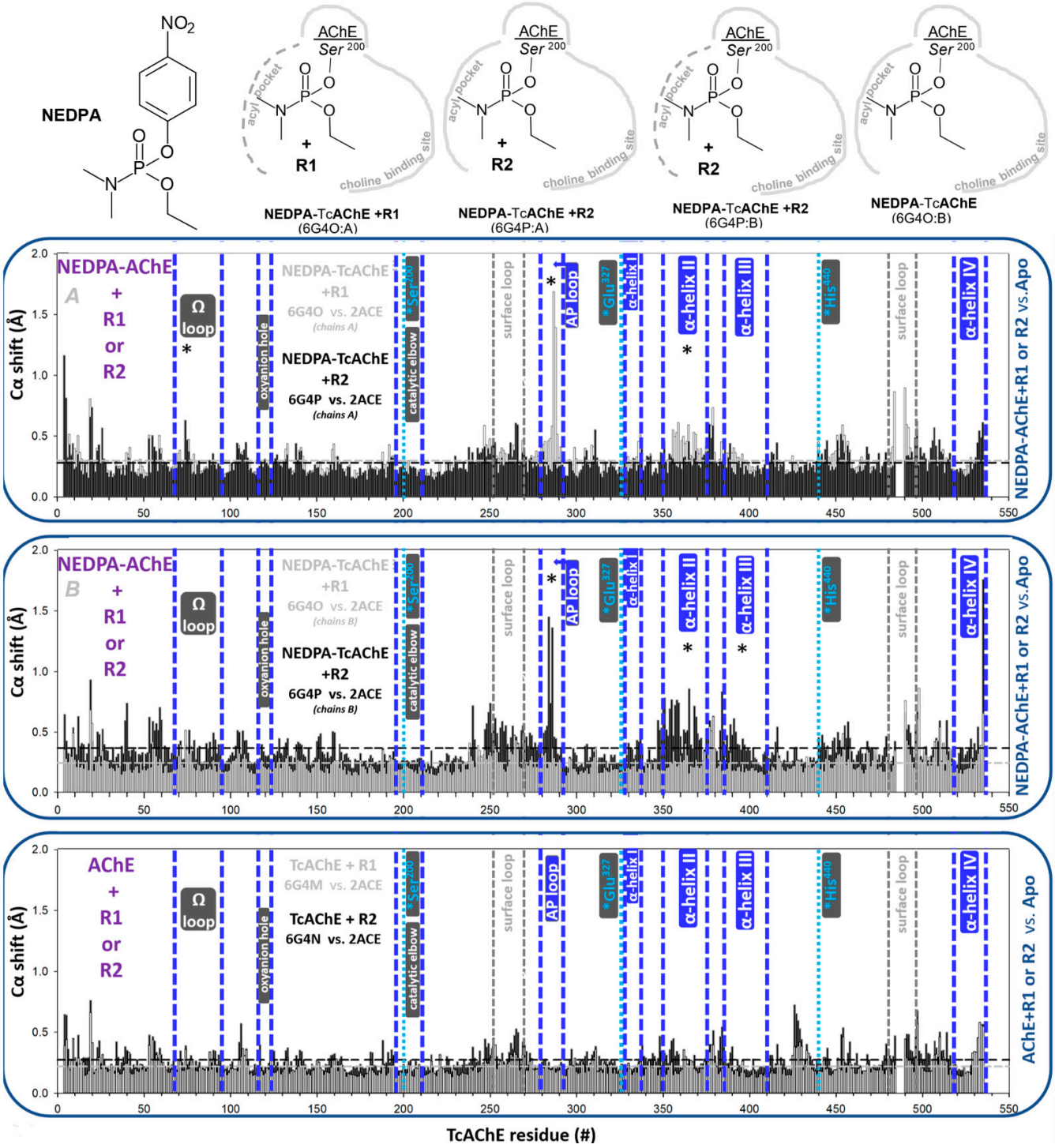

Figure 7. Structure of tabun analog NEDPA and schematic representation of its covalent binding to the active serine of TCAChE in the absence and the presence of oxime reactivators R1 and R2 [5]. Conjugates of NEDPA with AChE are identical to those formed by tabun. Schematics are based on X-ray structures of NEDPA-TcAChE conjugates, with PDB codes given in parentheses. Each structure contains chains A and B of the TcAChE homodimer in the asymmetric subunit. Monomers (chains) in homodimers show different conformations and were therefore analyzed by PACCT3 separately, with resulting data displayed in two separate bar charts. In bar charts, the alpha carbon shifts (in Å) of conjugated backbones are represented as vertical bars for each amino acid in the linear AChE sequence. Horizontal dashed lines indicate an average backbone atom shift, while stars indicate shifts considered significant. Functionally important structural elements of TcAChE are bracketed between vertical, dashed, and blue lines and labelled.

3.1.3. Covalent Conjugates Formed by Carbamates

The structures of carbamylated AChEs have been primarily studied with TcAChE. A largely planar configuration around covalently attached carbonyl carbon in carbamyl-AChE conjugates, compared to a tetrahedral configuration around covalently attached phosphorus in OP conjugates, seems to have an effect on the ability of substituents to be accommodated in the AP before the AP loop becomes distorted. For example, ethyl methyl-carbamylated TcAChE shows only small distortions of the AP loop backbone (Figure 8), compared to the much larger effect of the POX-inhibited hAChE (Figure 3) with similarly sized substituents (ethoxy group vs. ethyl methyl carbamyl group) accommodated in the pocket. The solvent accessible volume of the acyl pocket, at the same time, changes more significantly in the carbamylated TcAChE (Figure 9, panel C vs. panel A) and is similar to the effect in POX-hAChE (Figure 9, panel B vs. panel D) due to side-chain rotations. Nevertheless, the conformational flexibility of the AP loop backbone in carbamylated TcAChE remains large. Reversible binding of the above-mentioned uncharged reactivators R1 and R2 [5] to the peripheral site in TcAChE stabilizes the AP loop in two largely distorted conformations (Figure 7). Coincidentally, the positions of α-helices II are also clearly shifted, an effect already observed for OP-AChE conjugates. In addition, the most C-terminal α-helix IV shows notable shifts for the ethyl methyl carbamylated TcAChE (Figure 8).

The covalent binding of large monocarbamates, ganstigmine and MF268 to the active Ser200 of TcAChE appears to have no consequences on backbone conformations of TcAChE (Figure 8). Due to the larger rotational freedom in bonds of monocarbamates, they seem to achieve sterically fitting conformations inside the A easier than dicarbamates. In addition, the long aliphatic chain of MF268 seems to have sufficient intrinsic flexibility to avoid the steric obstacles of the narrow TcAChE active center gorge.

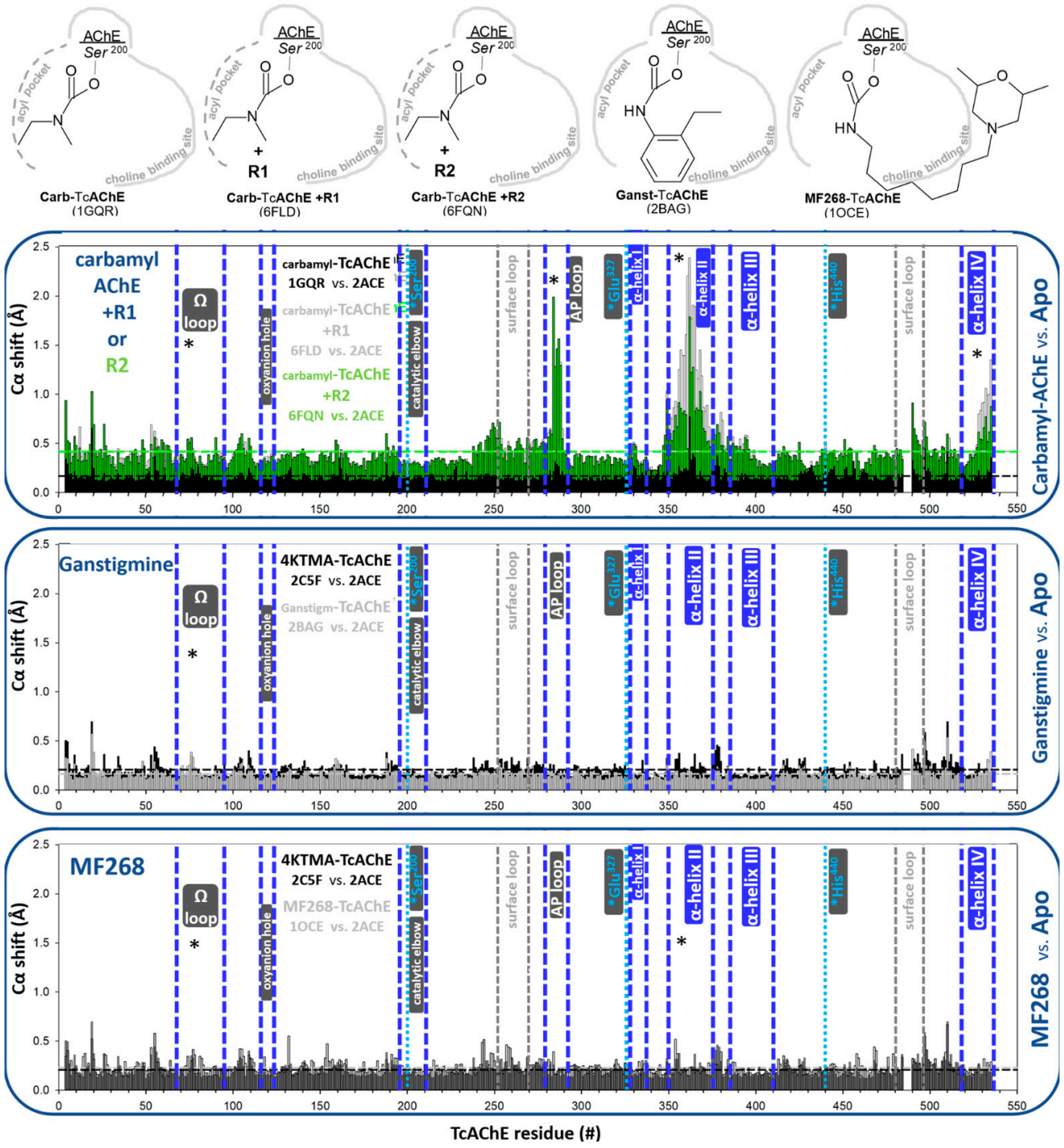

Figure 8. Schematic representation of TcAChE carbamylated by methyl ethylcarbamate, ganstigmine and carbamate MF268. Methylethylcarbamyl-TCAChE is shown in the presence of oxime reactivators R1 and R2 [5]. Schematics are based on X-ray structures with PDB codes given in parentheses. In bar charts, the alpha carbon shifts (in Å) of conjugated backbones are represented as vertical bars for each amino acid in the linear AChE sequence. Horizontal dashed lines indicate an average backbone atom shift, while stars indicate shifts considered significant. Functionally important structural elements of TcAChE are bracketed between vertical, dashed, and blue lines and labelled.

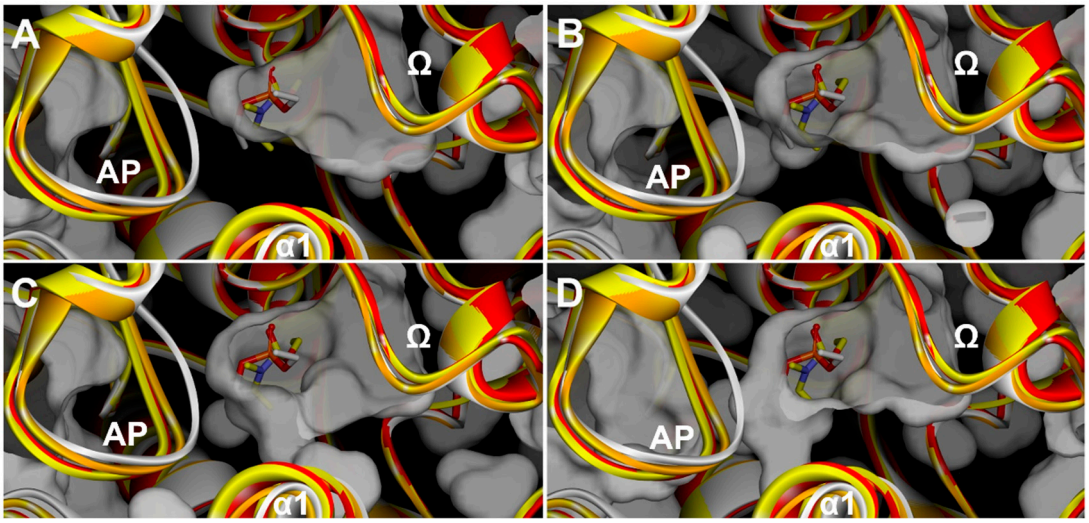

Figure 9. Comparative effects of ethyl methyl carbamylation of TcAChE and diethyl phosphorylation of hAChE on conformations of respective AP loops. Overlay of carbamyl-TcAChE (1GQR; yellow ribbon), apo-TcAChE (2ACE; red ribbon), POX-hAChE (5HF5; white ribbon), and apo-hAChE (4EY4; orange ribbon). Conjugated ethyl methylcarbamyl (yellow C atoms) and diethyl phosphoryl (white C atoms) entities are rendered as sticks. Shown are the Connolly surfaces of (**A**) Apo-TcAChE, (**B**) Apo-hAChE, (**C**) carbamyl-TcAChE and (**D**) POX-hAChE.

3.2. Effects of Reversible Binding on Backbone Conformation of hAChE

3.2.1. Reversible Binding of Substrates and Products

Structures of substrates of ACh, its thio analog ATCh and hydrolytic products Ch^-, TCh^- and Ac^- have been studied in complex with both TcAChE and mAChE [6,7]. The larger substrates BTCh and succinylcholine were studied only in complexes with mAChE [6]. While only a native, catalytically active enzyme was used in TcAChE studies, both a native and catalytically inactive Ser203Ala (S203A) mutant of mAChE was used. Crystallographic experiments contained all ligands in tens of mM to hundreds of mM concentrations, sufficient to allow them to form complexes in both the active center and in the peripheral site of AChEs, located at the rim of the active center gorge opening and adjacent to the Ω-loop. In all of those X-ray structures, the peripheral site was, therefore, occupied with a ligand, reflected in small shifts in the part of the Ω-loop (Figures 10 and 11). No other significant changes in Cα positions were observed except for shifts in α-helix II in the structure of the BTCh*mAChE complex, which were likely caused by an additional BTCh molecule bound from the outside to the surface of the enzyme molecule. This is reminiscent of the 4KTMA-AChE structures (Figure 1), except that in those tetrahedral conjugates, α-helix II was always slightly shifted. Both observations are consistent with the conclusion that conformations of AChEs observed in their apo states reflect conformations that are optimal for catalytic activity. Therefore, no conformational adjustments of the AChE backbone are needed when binding substrates to achieve the outstanding catalytic throughput of AChE.

On the other hand, the position of the covalently attached carbonyl carbon seems to have changed by ~0.8 Å from the acetylated form of TcAChE captured in 2HA5 to the tetrahedral form in conjugate with the transition state analogue 4KTMA (2HA0) in the direction of the choline binding site (Figure 12). Although slightly smaller in magnitude, this shift is analogous to the one observed for conjugated phosphorus in large OP-hAChE conjugates (Figure 4, [9]). It seems, therefore, that one of important properties of the choline binding site in AChEs is to attract and pull (and stabilize) large ester substituents, in both covalent inhibition and in the rapid catalytic cycle of an AChE.

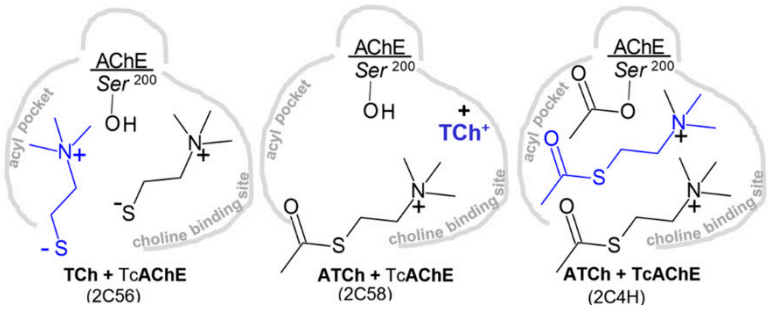

Figure 10. Structure of substrates ACh and ATCh and product TCh in reversible complexes with TcAChE. Schematics are based on X-ray structures, with PDB codes given in parentheses. Bar charts from PACCT3 analyses of each of three structures compared to the apo AChE (2ACE) are given in Figure S1.

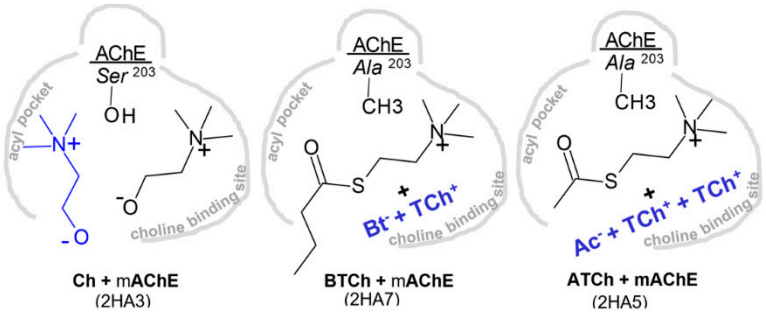

Figure 11. Structure of substrates ATCh and BTCh and product Ch in reversible complexes with mAChE. Schematics are based on X-ray structures with PDB codes given in parentheses. Bar charts from PACCT3 analyses of each of three structures compared to apo AChE (1J06) are given in Figure S2.

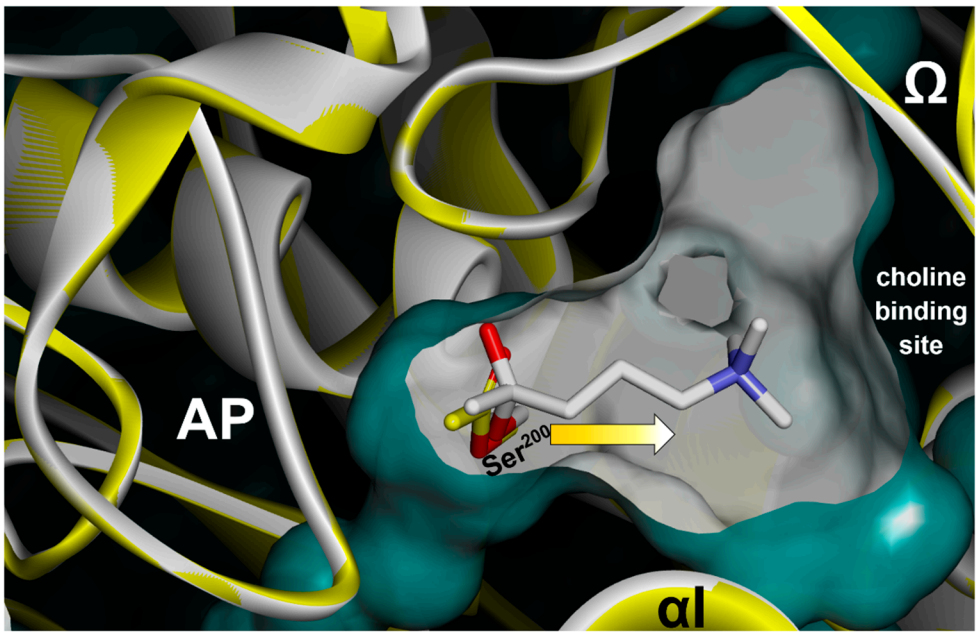

Figure 12. Shifts in position of the carbonyl carbon of the acetylated Ser^{200} of TcAChE (from 2C4H; yellow C atom sticks and yellow ribbon) towards the choline binding site (as indicated by the arrow) in the tetrahedral intermediate (4KTMA-TcAChE conjugate; white C atom sticks and white ribbon; 2C5F) by ~0.8 Å. Shown is the Connolly surface of the 2C4H cut-away to expose the active center gorge interior around active Ser200. Locations of the acyl pocket (AP), choline binding site, Ω-loop and α-helix I (αI) are indicated.

3.2.2. Reversible Binding of High-Affinity Inhibitors

While reversibly bound substrates, their hydrolytic products or transition state analogs, with high μM to mM binding affinity, do not induce notable changes in the backbone conformations of TcAChE and mAChE, a higher-affinity reversible ligand could have that capacity. The tightest binding of reversible ligands of AChEs are click-chemistry triazoles [17], created in situ within the AChE active center gorge and serving as a reaction vessel. Their binding affinities are in the fM concentration range. Due to the syn- vs. anti-isomerism of the triazole ring, a single pair of acetylene- and azide-decorated reactants can form either one of two isomers in situ (Figure 13). The highest affinity one is syn-TZ2PA6 (Figure 13), and TcAChE and mAChE, probably due to their intrinsically curved shape of the active center gorge channel, preferentially form syn-triazoles. There is a notable difference in the backbone configurations of structures of the syn- compared to anti-isomers (Figure 13). While anti-isomers practically do not affect the backbone conformation of mAChE, several orders of magnitude tighter-binding syn- isomers affect Ω-loop conformation and the conformations of α-helices II and I. Most of the Ω-loop distortions can also be observed in complexes with starting materials for the click-reaction (TZ2 and PA5; Figure 13). However, α-helix shifts are more pronounced in already formed syn-triazoles (both TZ2PA5 and TZ2PA6; Figure 13). It seems, therefore, that anti-triazoles bind best to the apo conformation of mAChE, and higher affinity syn-triazoles prefer mAChE of a slightly different backbone conformation.

Unlike high affinity triazoles that stabilize their tetrahydroacridine domains within the choline binding site and extend the phenantridinium ring system up the active center gorge towards its opening and the Ω-loop, picomolar inhibitor Tacrine-benzofuran extends its bi-cycle downwards, into the acyl pocket, near the base of the TcAChE active center gorge [18]. As a consequence, the conformation of the AP loop is severely distorted in this complex, with a significant shift of the α-helix II (Figure 14). This is likely due to a tight interaction between the benzofuran moiety with the aromatic residues of the AP pocket base, of the nature previously studied in other biological systems [19,20]. Backbone conformations of the Ω-loop or other relevant structural elements are not affected. The magnitude of the AP loop shift is larger than what was previously reported for bis-tacrine5 [21], another tacrine-based reversible inhibitor (Figure S3). While the choline binding site stabilizes the tetrahydroacridine moiety similarly in both compounds, the second tetrahydroacridine of bis-tacrine5 interacts with the concave part of the AP loop in a way that is similar to the interaction of R2 (Figure 8). Both R2 and bis-tacrine5 stabilize a similarly distorted conformation of the AP loop. In addition, the effect of bis-tacrine5 on the α-helix II shift is even larger than the one observed for tacrine-benzofuran (Figures 14 and S3). Taken together, this is another example where shifts in the α-helix II are inflicted indirectly via an AP loop interaction, since neither ligand makes direct contact with the helix. The assumption of connectivity of the two structural elements (the AP loop and C-terminal α-helix II) in the direction of the lower part of the active center gorge towards the enzyme's C-terminus (where the homo-dimerization interface is located), thus holds for reversible ligands, as well.

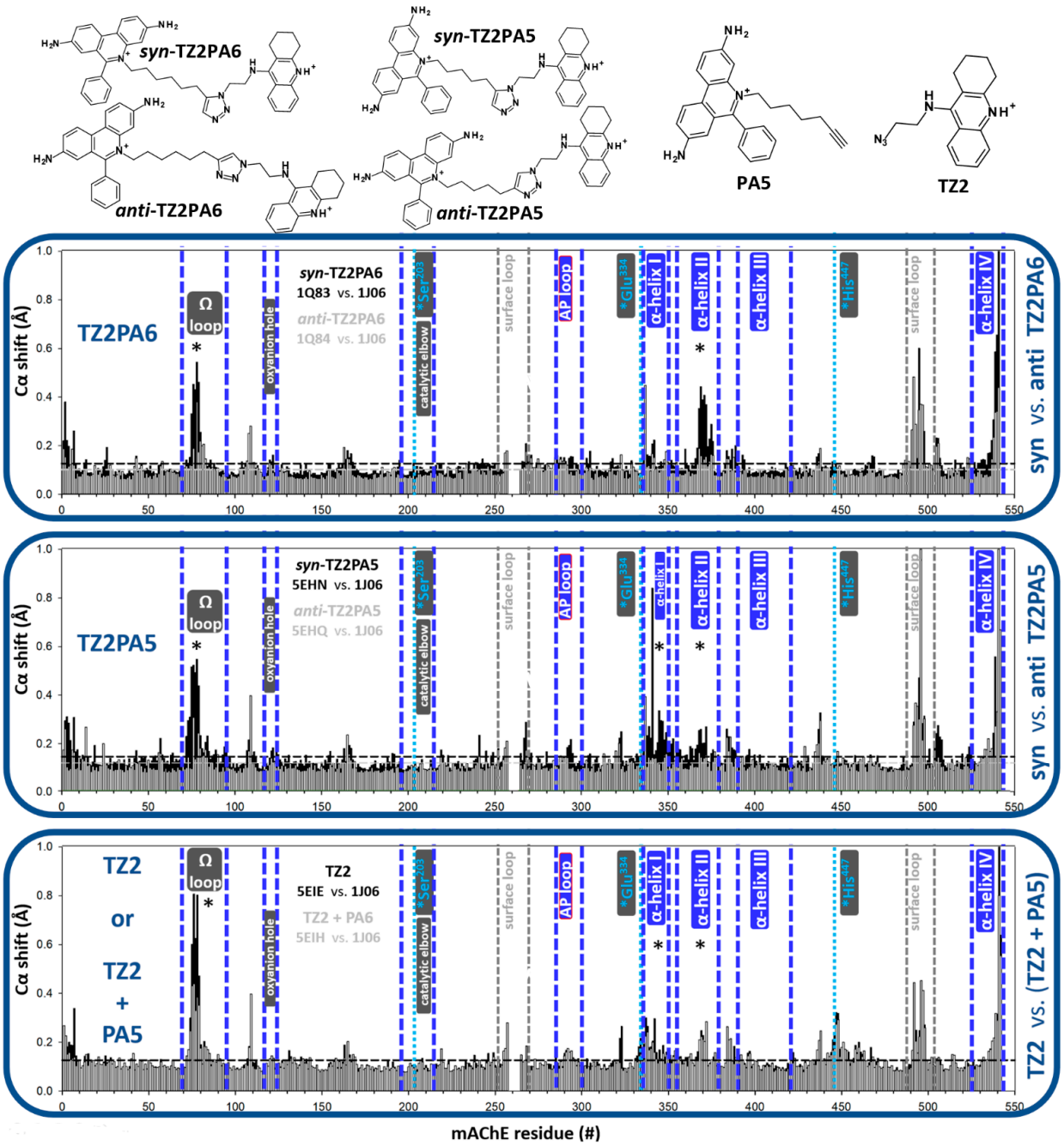

Figure 13. Structures of tight-binding, reversible, triazole inhibitors of AChE. Syn- and anti-isomers differ by several orders of magnitude in their binding affinities. TZ2 and PA6 are the starting materials for the in situ click-chemistry synthesis of triazoles. Compounds are shown in protonation states predominant at the physiological pH 7.4. Bar charts are from PACCT3 analyses of each of six structures compared to the apo AChE (1J06). Alpha carbon shifts (in Å) of conjugated backbones are represented as vertical bars for each amino acid in the linear AchE sequence. Horizontal dashed lines indicate an average backbone atom shift, while stars indicate shifts considered significant. Functionally important structural elements of hAChE, bracketed between vertical, dashed, blue lines and labelled, are mapped within the 3D structure of hAChE in Figure 2.

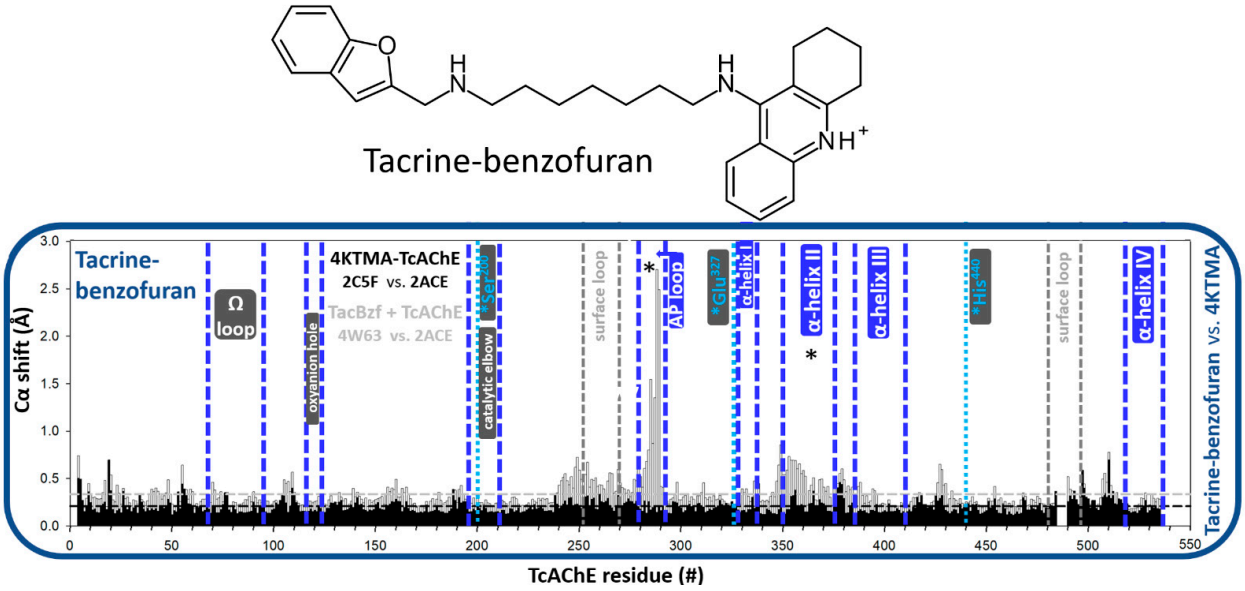

Figure 14. Structure of tacrine-benzofuran, a pM reversible inhibitor of TcAChE. Bar charts from PACCT3 analyses of the reversible complex X-ray structure compared to the apo AChE (2ACE). Parallel comparison of 4KTMA-TcAChE conjugate vs. apo TcAChE (2ACE) is given as a frame of reference. The compound is shown in protonation states predominant at the physiological pH 7.4. Alpha carbon shifts (in Å) of conjugated backbones are represented as vertical bars for each amino acid in the linear AChE sequence. Horizontal dashed lines indicate an average backbone atom shift, while stars indicate shifts considered significant. Functionally important structural elements of hAChE are bracketed between vertical, dashed, and blue lines and labelled.

4. Discussion

The present study presented pairwise analyses of changes in the Cα backbone conformations of non-liganded hAChE, mAChE and TcAChE upon their interaction with reversible and covalent ligands, providing evidence for several function-related properties of AChE's structure.

In interactions with physiological and closely related substrates (Ach, ATCh, BTCh), and, in particular, with the tetrahedral transition state analog 4KTMA, no significant alterations of the Cα backbone conformations were observed, suggesting that conformations of the apo forms of AchEs determined by X-ray diffraction generally reflect an optimal geometry evolved for its highly advanced catalytic mechanism. This is also consistent with our previous room-temperature X-ray crystallography of the 4KTMA-hAChE conjugate, which revealed a basically unchanged conformation of the hAChE backbone in diffraction data collected at either 100 K or 293 K [10].

The effects of a larger diversity of tetrahedral conjugate geometries on backbone conformations in AChEs are revealed through the investigation of OP esters that dephosphorylate very slowly and are thus amenable for X-ray structure determination. In principle, whenever a substituent larger than two carbons (the equivalent of a propionyl substituent in propionylcholine) is directed into the AP from the P atom tethered to the active Ser by a covalent bond and by phosphonyl oxygen stabilization in the oxyanion hole, the conformation of the AP loop is distorted. This is demonstrated for POX-hAChE and DFP-AChEs in both aged and non-aged conjugates, as well as in tabun-AChEs (NEDPA-AChE) and R_PVX-hAChE. A notable exception is A234-hAChE, a Novichok conjugate where AP loop distortion is avoided by the 1.0–1.5 Å shift of the conjugated OP towards the choline binding site. A property of the latter site to attract and pull suitable entities tethered to the active Ser is revealed even for OP conjugates with small AP-directed substituents, such as VX, soman and A230 (Figure 3). The presence of phosphorus in soman and A230 causes a shift in those conjugates of 0.5–0.6 Å compared to VX. Due to the larger size of their ester substituents directed towards the choline binding site, they have a better

potential for tighter hydrophobic stabilization within that site. A similar 0.8 Å shift of the Ser-conjugated carbonyl carbon can be seen in a comparison of the acetyl-TcAChE and 4KTMA-TcAChE conjugates (Figure 12), where the much larger "choline-like" quaternary ammonium entity of 4KTMA fits snugly into the TcAChE choline binding site by virtue of a cation-Π interaction. The choline binding site thus seems to have the function of not only directing, but also of pulling and "stretching-out" Ser-conjugated entities for more optimal catalysis. On the other hand, the conformation of the AP loop does not seem to be rigid to the extent of steric expulsion of large substituents. It is, for example, flexible enough to distort its conformation in the aged POX-hAChE or DFP-AChEs, with no or with minimal shifts of conjugated phosphorus in the direction of the choline binding site. Dealkylation-generated sizeable empty spaces within the choline binding site thus remain unoccupied, while on the other side, the AP loop is distorted, with a seemingly small energy cost. While the binding of reversible ligands, such as oximes 2PAM or HI6, can revert a distorted AP loop into its native conformation, certain ligands that can either fit into the occupied AP or bind within the concave part of the AP loop have the capacity to stabilize and further potentiate distortion, as observed for SP134 and reactivators R1 and R2 bound to tabun (or NEDPA)-TcAChE conjugates.

Shifts of C-terminal α-helices are always observed alongside distortion of the AP loop, revealing an important connectivity that could lead to a component of an allosteric interaction. Those shifts, however, are typically not reverted upon reversible ligand binding.

The planar geometry around the atom conjugated to Ser, found in acetylated-TcAChE but also in carbamyl-TcAChE conjugates, results in similar AP loop distortions for large substituents, such as for ethyl methyl carbamate resulting from inhibition by rivastigmine. The same mentioned reactivators, R1 and R2, further potentiate this distortion, as in tabun-TcAChE conjugates. Connectivity with C-terminal α-helices is again observed. The large mono-substituted carbamates, ganstigmine and MF268, however, direct their substituents away from the AP loop, and thus, do not inflict distortion and do not affect the shift in the C-terminal α-helices.

Finally, into the emerging picture of a flexible AP loop, connected C-terminal α-helices and an attracting choline binding site, the non-covalent complexation of tight binding inhibitors fits well. Complexes of different triazole isomers prefer slightly different conformations of mAChE in the Ω-loop and C-terminal α-helices, while tacrine-benzofuran in direct contact with the AP loop stabilizes its distorted conformation and indirectly induces C-terminal α-helical shifts.

In conclusion, the analysis of backbone conformations in X-ray structures of three AChEs (hAChE, mAChE and TcAChE) interacting with diverse ligands reveals the AP loop backbone conformation as the most responsive and conformationally diverse of all structural elements of the AChE backbone. Structural changes in this loop located in the immediate vicinity of the catalytic triad Ser practically always coincide with shifts of one or more C-terminally located α-helices with the capacity to establish connectivity that could result in an allosteric interaction. AP loop conformations do not appear to be rigid and sterically exclusive, but rather adjustable around both small and large interacting ligands. The stabilizing potential of the choline binding site, on the other side of the active center gorge, on the other hand, acts as an attractant for large hydrophobic and cationic entities that can pull them out of the spatially restricted AP and relieve overall compaction within the active center gorge of AChEs. It is reasonable to assume that, in solution, the magnitudes of conformational freedom and the described interactions increase, representing significant constraints in the structure-based design of both therapeutical inhibitors and reactivators of already inhibited AChEs.

Supplementary Materials: The following are available online at https://www.mdpi.com/article/10.3390/cryst11121557/s1, Figure S1: Analysis of substrates ACh and ATCh and product TCh in reversible complexes with TcAChE. Figure S2: Analysis of substrates ATCh and BTCh and product Ch in reversible complexes with mAChE, Figure S3: Analysis of Bis-Tacrine5 reversibly bound to TcAChE.

Funding: This research was supported by the CounterACT Program, National Institutes of Health Office of the Director (NIH OD), the National Institute of Neurological Disorders and Stroke (NINDS), [Grant Numbers U01 NS083451 and R21 NS098998] and by the UCSD Academic Senate grant BG084144.

Data Availability Statement: All data are contained within the manuscript or are available to be shared upon request (please contact the author).

Conflicts of Interest: The author declares no conflict of interest.

References

1. Quinn, D.M. Acetylcholinesterase: Enzyme structure, reaction dynamics, and virtual transition states. *Chem. Rev.* **1987**, *87*, 955–979. [CrossRef]
2. Sussman, J.L.; Harel, M.; Frolow, F.; Oefner, C.; Goldman, A.; Toker, L.; Silman, I. Atomic structure of acetylcholinesterase from Torpedo californica: A prototypic acetylcholine-binding protein. *Science* **1991**, *253*, 872–879. [CrossRef] [PubMed]
3. Radić, Z.; Taylor, P. Structure and Function of Cholinesterases. In *Toxicology of Organophosphate and Carbamate Compounds*; Gupta, R.C., Ed.; Elsevier: San Diego, CA, USA, 2006.
4. Franklin, M.C.; Rudolph, M.J.; Ginter, C.; Cassidy, M.S.; Cheung, J. Structures of paraoxon-inhibited human acetylcholinesterase reveal perturbations of the acyl loop and the dimer interface. *Proteins* **2016**, *84*, 1246–1256. [CrossRef] [PubMed]
5. Santoni, G.; de Sousa, J.; de la Mora, E.; Dias, J.; Jean, L.; Sussman, J.L.; Silman, I.; Renard, P.Y.; Brown, R.; Weik, M.; et al. Structure-Based Optimization of Nonquaternary Reactivators of Acetylcholinesterase Inhibited by Organophosphorus Nerve Agents. *J. Med. Chem.* **2018**, *61*, 7630–7639. [CrossRef] [PubMed]
6. Bourne, Y.; Radić, Z.; Sulzenbacher, G.; Kim, E.; Taylor, P.; Marchot, P. Substrate and product trafficking through the active center gorge of acetylcholinesterase analyzed by crystallography and equilibrium binding. *J. Biol. Chem.* **2006**, *281*, 29256–29267. [CrossRef] [PubMed]
7. Colletier, J.P.; Fournier, D.; Greenblatt, H.M.; Stojan, J.; Sussman, J.L.; Zaccai, G.; Silman, I.; Weik, M. Structural insights into substrate traffic and inhibition in acetylcholinesterase. *EMBO J.* **2006**, *25*, 2746–2756. [CrossRef] [PubMed]
8. Radić, Z.; Pickering, N.A.; Vellom, D.C.; Camp, S.; Taylor, P. Three distinct domains in the cholinesterase molecule confer selectivity for acetyl- and butyrylcholinesterase inhibitors. *Biochemistry* **1993**, *32*, 12074–12084. [CrossRef] [PubMed]
9. Luedtke, S.; Bojo, C.; Li, Y.; Luna, E.; Pomar, B.; Radić, Z. Backbone Conformation Shifts in X-ray Structures of Human Acetylcholinesterase upon Covalent Organophosphate Inhibition. *Crystals* **2021**, *11*, 1270. [CrossRef]
10. Gerlits, O.; Blakeley, M.P.; Keen, D.A.; Radić, Z.; Kovalevsky, A. Room temperature crystallography of human acetylcholinesterase bound to a substrate analogue 4K-TMA: Towards a neutron structure. *Curr. Res. Struct. Biol.* **2021**, *3*, 206–215. [CrossRef] [PubMed]
11. Blumenthal, D.K.; Cheng, X.; Fajer, M.; Ho, K.Y.; Rohrer, J.; Gerlits, O.; Taylor, P.; Juneja, P.; Kovalevsky, A.; Radić, Z. Covalent inhibition of hAChE by organophosphates causes homodimer dissociation through long-range allosteric effects. *J. Biol. Chem.* **2021**, *297*, 1–14. [CrossRef]
12. Rohrer, J.; Sidhom, M.; Han, J.; Radić, Z. Overlay-independent comparisons of X-ray structures reveal small, systematic conformational changes in liganded acetylcholinesterase. *Period. Biol.* **2016**, *118*, 319–328. [CrossRef]
13. wwPDB Consortium. Protein Data Bank: The single global archive for 3D macromolecular structure data. *Nucleic Acids Res.* **2019**, *47*, D520–D528. Available online: https://pubmed.ncbi.nlm.nih.gov/30357364/ (accessed on 10 December 2021). [CrossRef] [PubMed]
14. Cheung, J.; Rudolph, M.J.; Burshteyn, F.; Cassidy, M.S.; Gary, E.N.; Love, J.; Franklin, M.C.; Height, J.J. Structures of human acetylcholinesterase in complex with pharmacologically important ligands. *J. Med. Chem.* **2012**, *55*, 10282–10286. [CrossRef] [PubMed]
15. Taylor, P.; Wong, L.; Radić, Z.; Tsigelny, I.; Brüggemann, R.; Hosea, N.A.; Berman, H.A. Analysis of cholinesterase inactivation and reactivation by systematic structural modification and enantiomeric selectivity. *Chem. Biol. Interact.* **1999**, *119–120*, 3–15. [CrossRef]
16. Hörnberg, A.; Tunemalm, A.K.; Ekström, F. Crystal structures of acetylcholinesterase in complex with organophosphorus compounds suggest that the acyl pocket modulates the aging reaction by precluding the formation of the trigonal bipyramidal transition state. *Biochemistry* **2007**, *46*, 4815–4825. [CrossRef] [PubMed]
17. Lewis, W.G.; Green, L.G.; Grynszpan, F.; Radić, Z.; Carlier, P.R.; Taylor, P.; Finn, M.G.; Sharpless, K.B. Click chemistry in situ: Acetylcholinesterase as a reaction vessel for the selective assembly of a femtomolar inhibitor from an array of building blocks. *Angew. Chem. Int. Ed. Engl.* **2002**, *41*, 1053–1057. [CrossRef]
18. Zha, X.; Lamba, D.; Zhang, L.; Lou, Y.; Xu, C.; Kang, D.; Chen, L.; Xu, Y.; Zhang, L.; De Simone, A.; et al. Novel Tacrine-Benzofuran Hybrids as Potent Multitarget-Directed Ligands for the Treatment of Alzheimer's Disease: Design, Synthesis, Biological Evaluation, and X-ray Crystallography. *J. Med. Chem.* **2016**, *59*, 114–131. [CrossRef] [PubMed]
19. Baykov, S.V.; Mikherdov, A.S.; Novikov, A.S.; Geyl, K.K.; Tarasenko, M.V.; Gureev, M.A.; Boyarskiy, V.P. π–π Noncovalent Interaction Involving 1,2,4- and 1,3,4-Oxadiazole Systems: The Combined Experimental, Theoretical, and Database Study. *Molecules* **2021**, *26*, 5672. [CrossRef] [PubMed]

20. Kryukova, M.A.; Sapegin, A.V.; Novikov, A.S.; Krasavin, M.; Ivanov, D.M. New Crystal Forms for Biologically Active Compounds. Part 1: Noncovalent Interactions in Adducts of Nevirapine with XB Donors. *Crystals* **2019**, *9*, 71. [CrossRef]
21. Rydberg, E.H.; Brumshtein, B.; Greenblatt, H.M.; Wong, D.M.; Shaya, D.; Williams, L.D.; Carlier, P.R.; Pang, Y.P.; Silman, I.; Sussman, J.L. Complexes of alkylene-linked tacrine dimers with Torpedo californica acetylcholinesterase: Binding of Bis5-tacrine produces a dramatic rearrangement in the active-site gorge. *J. Med. Chem.* **2006**, *49*, 5491–5500. [CrossRef] [PubMed]